Bottle-to-Bottle Recycling of PET Via Nanostructure Formation by Melt Intercalation in Twin Screw Compounder: Improved Thermal, Barrier, and Microbiological Properties

Sh. Hamzehlou, A. A. Katbab

Polymer Engineering Faculty, AmirKabir University of Technology, Tehran, Iran

Received 5 February 2006; accepted 4 April 2007
DOI 10.1002/app.26730
Published online 12 July 2007 in Wiley InterScience (www.interscience.wiley.com).

ABSTRACT: Attempts have been made to modify the properties of the injection processing-scraped PET (denoted as RPET) via intercalation with different levels of organically modified nanoclay (montmorillonite) by melt blending in a corotating twin screw compounder. The clay platelets dispersion state has been qualitatively correlated with the melt linear viscoelastic as well as tensile and barrier properties of the prepared nanocomposites. Oxygen permeation of the nanocomposite PET films showed significant reduction compared with the pristine PET polymer. All the PET/nanoclay composites exhibited no bacterial growth, with no potentiality to generate acetaldehyde, as measured by GC/Mass analyzer. X-ray diffractometry and transmission electron microscopy performed on the scraped PET/organoclay nanocomposite samples showed increase in d_{001} spacing of the clay layers and their dispersion throughout the PET matrix. Differential scanning calorimetry analysis showed higher crystallization temperature as well as crystallization enthalpy (ΔH_c) for the nanocomposite samples, compared with the unprocessed virgin PET. The RPET nanocomposite samples composed of 3 and 5% of nanoclay exhibited enhanced melt elastic modulus and pseudosolid-like behavior at low shear frequencies measured by rheomechanical spectroscopy than the unfilled pristine-scraped PET, indicating the formation of nanoscopic network structure by the clay platelets, which leads to the development of nanostructured resin. © 2007 Wiley Periodicals, Inc. J Appl Polym Sci 106: 1375–1382, 2007

Key words: nanocomposites; recycling; PET; organoclay; melt intercalation

INTRODUCTION

Polyethylene terephthalate (PET) is one of the polymeric materials with low cost and high performance that has been widely used in various engineering applications such as in textile, reinforcement of tires, food and beverage packaging (water soft drink bottles).[1,2] Food and beverage application of PET resin has seen enormous growth over the last 20 years, and continues to enjoy increasing popularity. However, from an ecological point of view, there has been a worldwide attempt to reduce the environmental influences caused by the disposed PET products by reusing and recycling of these materials. Bottle-to-bottle recycling of PET has become a major issue in most countries. However, PET undergoes thermal and hydrothermal degradation, which leads to the decrease in its molecular weight (MW) and mechanical and gas-barrier properties. This makes its recycling via melt processing problematic, and therefore reduces its application potential to be remolded into the products by using the processes in which high melt strength is required. Note that the PET bottles are manufactured by stretch-blow molding of a preform tube which needs high melt strength. PET is very sensitive to heat in the presence of moisture, acidic, and also causting components which might exist as contaminant agents.

To overcome these shortcomings, different modification methods have been employed, such as blending with a rubbery material,[3–5] and solid state polymerization (SSP). In SSP technique, the MW [characterized by the intrinsic viscosity (IV)] is enhanced by keeping the recycled PET at high temperature in an oxygen and moisture-free environment. This process leads to a prolonged polycondensation of PET. However, although this is an efficient but time-consuming process, researches have been looking for other effective processes such as chain extending methods.[6–10] There have been many approaches to improve the gas-barrier properties of recycled and postconsumed PET. These include incorporating the PET with aromatic monomers,[11] talc and layered fillers,[12] blending with thermoplastic liquid crystalline

Correspondence to: A. A. Katbab (katbab@aut.ac.ir).
Contract grant sponsor: Industrial Development and Renovation Organization of Iran (IDRO).

Journal of Applied Polymer Science, Vol. 106, 1375–1382 (2007)

polymer,[13] and treatment of the PET film surface with plasma. However, none of these methods has been industrially promising as the clarity of PET is reduced.

During the last few years, polymer/clay nanocomposites have attracted great attention from the academic and industrial point of view to enhance the properties of polymers, including improved strength modulus, increased thermal stability, and reduced gas permeability, with high transparency compared with the pure polymer.[14–16] In the process of melt mixing, the layered silicate (nanoclay) is compounded with the molten polymer matrix. Depending on the compatibility of the polymer with the nanometric silicate layers, the polymer can diffuse into the gallery space of the nanoclay, forming intercalated or exfoliated type of microstructure. In the exfoliated structure, the silicate layers are completely delaminated or opened up, and dispersed disorderly and uniformly throughout the continuous polymer matrix. This leads to the high filler aspect ratio that results in enhanced interaction between the polymer and the dispersed layers, and consequently reinforcement of the melt strength and all other properties. It is expected that dispersing the organomodified montmorillonite into the PET matrix would result in the enhancement of the melt strength, modulus, heat distortion temperature, and decrease in gas permeability, while retaining the transparency.

In the present work, attempts have been made to improve the properties, thermal stability, and melt strength of recycled PET bottles by melt intercalation with a specific organomodified montmorillonite for the purpose of being transferred back into the bottle production line.

EXPERIMENTAL

Material

Bottle-grade PET resin with the commercial name of ASPET21C made by M. Bendi, India, was provided by Zam-Zam soft drink Company of Iran. This resin had an IV of 0.81 dL/g in a solution prepared by dissolving 1 kg of phenol in 510 mL of 1,2-dichlorobenzene measured at 30°C with an Ubbelohde viscometer. Scraped PET resin, which has been denoted as RPET, was the flash PET remained at the gate of the injection mold during preform manufacturing by injection molding process of the virgin PET. The used processing-scraped PET (RPET) had IV of 0.76 dL/g. The layered silicate used in this work was a montmorillonite modified with methyl tallow bis(2-hydroxyethyl) ammonium and kindly supplied by Zhejiang FengHong Clay Co. (China) with the commercial name of DK2. This organomodified clay had d_{001} basal spacing of 27.68, 18.62 Å (distance between layers), with a cation exchange capacity of 120 mequiv/100 g, and average dry particle size of less than 50 μm.

Preparation of PET/MMT nanocomposite

Prior to mixing, both PET and organomodified nanoclay (DK2) was dried in a vacuum oven at 120 and 80°C, respectively, for 24 h to prevent moisture-induced thermal degradation of PET. Nanocomposites were prepared by melt compounding of PET and nanoclay in a twin screw compounder model Brabender Plastic Corder DSE20 with $L/D = 40$. The die temperature and screw speed were set at 250°C and 100 rpm, respectively. For the purpose of comparison, the virgin PET was also processed inside the compounder under the same conditions that nanocomposite samples were prepared, and identified as PPET.

Characterization

To evaluate the degree of interaction between the PET matrix and nanoclay (intercalation and/or exfoliation), wide-angle X-ray diffraction patterns were obtained by the use of Phillips X-ray diffractometer (XRD) model X-Pert with a wavelength of Cu Kα = 1.54 Å at 30 kV and 30 mA, at a scanning rate of 0.1° (2θ)/min. The patterns were recorded from 1.5° to 10° (2θ). A transmission electron microscopy (TEM) model JEOL 1200 EX was employed to evaluate the degree of separation and dispersion of the nanoclay layers onto the PET matrix, using ultra thin sections with a thickness of 100 nm prepared by microtoming frozen plates using an ultrahigh microtome. The IV of the samples was measured by the Zimmer method using a Lauda E100 Ubbelohde viscometer. For this purpose, the sample was dissolved in a mixture of 1 kg phenol/510 mL 1,2-dichlorobenzene, and the measurement was carried out at 25°C. Permeability of the prepared samples toward oxygen was measured according to the ASTM 1434-82 using a GDP-C permeability tester. Thermal stability was also studied using a Perkin-Elmer Pyris-1 thermogravimetric analyzer at a heating rate of 10°C/min. Differential scanning calorimetry (DSC) model TA was employed to evaluate the thermal behavior and thermophysical parameters such as melting point (T_m), glass transition temperature (T_g), and crystallization temperature (T_c), as well as degree of crystallinity of the samples. For this purpose, 5–7 mg samples were dried at 80°C for 4 h in a vacuum oven before DSC characterization, and thermograms were obtained by heating the samples at the rate of 5°C/min to 280°C, and autocooled at 5°C/min. T_m was considered to be the maximum of the endothermic melting peak of the thermogram, and T_c that of the exothermic peak

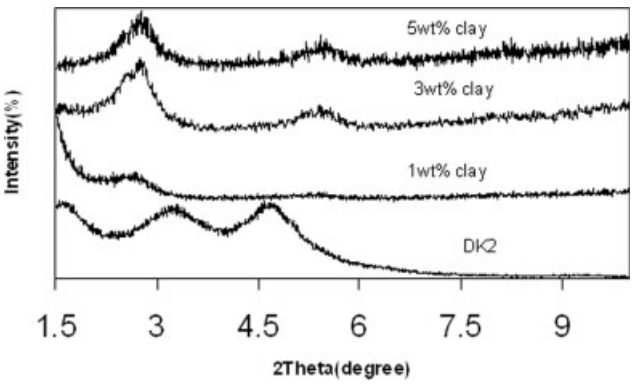

Figure 1 XRD patterns of Nanoline (DK2) and virgin PET/DK2 nanocomposite samples.

of the crystallization from the cooling scan. The heat of fusion (ΔH_f) and degree of crystallinity were measured from the area of the melting and crystallization peaks. All data are the average of three subsequent measurements. Acetaldehyde content of the samples was measured in a GC/Mass spectrometer model HP6890/5973 with an auto headspace sampler model HP7694. Tensile properties were also evaluated by a tensometer model Monsanto T500, using test specimens in the shape of strips with the dimensions of 20 × 200 mm^2 cut from a sheet, with a thickness of 0.3 mm and extension rate of 50 mm/min. Finally, the microbiological characteristics of the prepared nanocomposite samples were assessed by bacterial culture method. This was carried out by putting each sample in a suspension solution composed of *Staphylococcus* and *Escherichia coli* as hot-positive and hot-negative bacteria, respectively, for 24 h. After this period, the number of the attached bacterias was counted according to the standard plate count–pour plate method. The melt viscoelastic properties of the RPET and its corresponding nanocomposites were studied using rheometric mechanical spectrometer (RMS) model Paar Physica US200, parallel plate. All measurements were carried out at 265°C, within the frequency range of 0.1–1000 rad/s and a strain amplitude of 1%, which was found to be within the linear viscoelastic region of the samples.

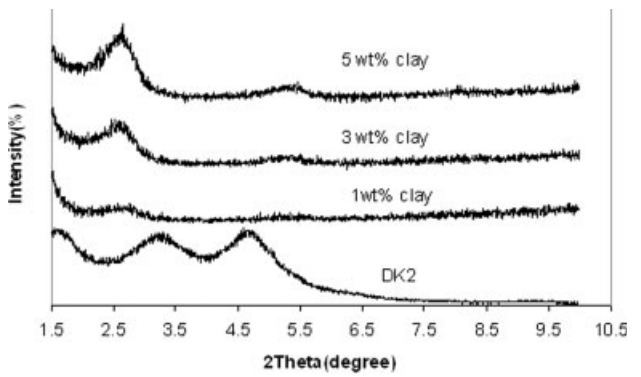

Figure 2 XRD patterns of Nanoline (DK2) and RPET/DK2 nanocomposite samples.

RESULTS AND DISCUSSION

The extent of intercalation (intercalation and exfoliation) between the nanoclay and virgin PET as well as RPET matrices have been demonstrated in the WAXD patterns of different samples given in Figures 1 and 2. The d_{001} diffraction peaks of the organoclay (DK2) have appeared at $2\theta = 3.18^\circ$ and 4.74°, which corresponds to an interlayer distances of 27.68 and 18.62 Å, respectively. It is clearly seen that, for all the nanocomposite PET samples, the d_{001} diffraction peaks of the nanoclay DK2 ($2\theta = 3.18^\circ$ and 4.74°) have been shifted to the lower angle, indicating the intercalation of the PET chains in between the gallery spaces of the nanoclay layers. TEM micrograph of the nanocomposite sample containing 3 wt % nanoclay at a magnification of 100,000 has also been presented in Figure 3. The presence of nanoclay platelets with the thickness of 4 nm in the PET matrix obviously seem as dark parallel lines separated from each other, which evidences the intercalation and exfoliation of clay nanolayers by the PET molecules.

The lower viscosity of the RPET than the virgin PET, as presented in Table I, enhances the interdiffusion of the RPET chains into the gallery spaces of the nanoclay layers. However, when the content of the DK2 is increased to 5%, the d_{001} diffraction peak shifts to the lower angle with higher intensity than the 3.18° (2θ) peak of the pristine DK2, which indicates that the PET chains have mainly intercalated in between the nanoclay layers. The domination of

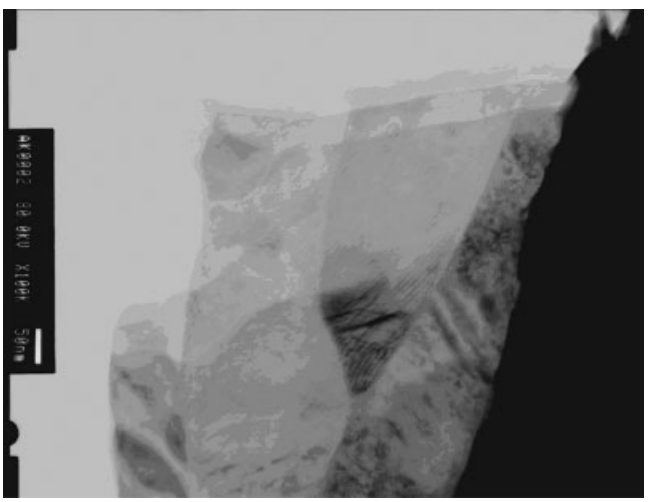

Figure 3 TEM micrograph of processing scraped PET/clay nanocomposite sample composed of 3 wt % of nanoclay (DK2).

TABLE I
Intrinsic Viscosity of Nano-PET

Sample	Intrinsic viscosity (dL/g)
FPET	0.819
Processed PET	0.792
PET + 1 wt % clay	0.800
PET + 3 wt % clay	0.722
PET + 5 wt % clay	0.646
RPET	0.760
Processed RPET	0.618
RPET + 1 wt % clay	0.657
RPET + 3 wt % clay	0.652
RPET + 5 wt % clay	0.636

intercalation type of nanostructure observed earlier for the nanoclay concentration of 3% could be related to the percolation of the clay particles, where a mesoscopic network structure is formed.[17]

The IV of the nanocomposite PET samples based on virgin and RPET resin has been shown and compared with the corresponding PET samples subjected to the same thermomechanical history in Table I. It is observed that for both groups inclusion of organoclay (DK2) into the matrix of the PET leads to the decrease of the IV, as well as the MW of the resin. However, the decrease in the IV by increasing the content of the organoclay is insignificant when RPET is compounded compared with the virgin unprocessed PET resin.

The heating and cooling DSC thermograms obtained for the processed RPET (PRPET) and RPET/nanocomposite samples have been exhibited in Figure 4(a,b), respectively. DSC thermogram of the virgin PET has also been exhibited in Figure 5. The values of the thermophysical parameters (T_g, T_m, T_c, ΔH_m, ΔH_c) determined from this experiment have also been presented in Table II. It is evident that all the RPET/nanocomposite samples, which were quenched immediately after leaving the compounder die, show a distinct crystallization peak within a temperature range above their glass transition temperature during the heating process. However, this peak has not appeared in the heating thermogram of the virgin PET as its structure was already crystalline. Therefore, the thermal behavior of the virgin PET during heating process should not be compared with those of the RPET/nanocomposites. The RPET/nanocomposites show higher values for the heat of fusion (ΔH_m) than the PRPET, which indicates the nucleating action of the nanoline particles and its platelets, leading to the higher degree of crystallinity.

Higher glass transition temperature (T_g) detected for the RPET nanocomposite sample composed of 1–3% by weight of nanoline (DK2) is attributed to the interfacial interaction between the nanoclay platelets and PET segments. Lower T_g value for the 5% nanocomposite sample is due to the more reduction of the PET MW by the nanoclay (Table I). However, the DSC thermograms recorded for the virgin PET, PRPET and its corresponding nanocomposites during the cooling scan of the melt show a distinct exothermic crystallization peak. It is clearly seen that the exothermic nonisothermal crystallization peak of the virgin PET has appeared as a wide curve with a peak temperature (T_c) of 164.84°C, and onset crystal-

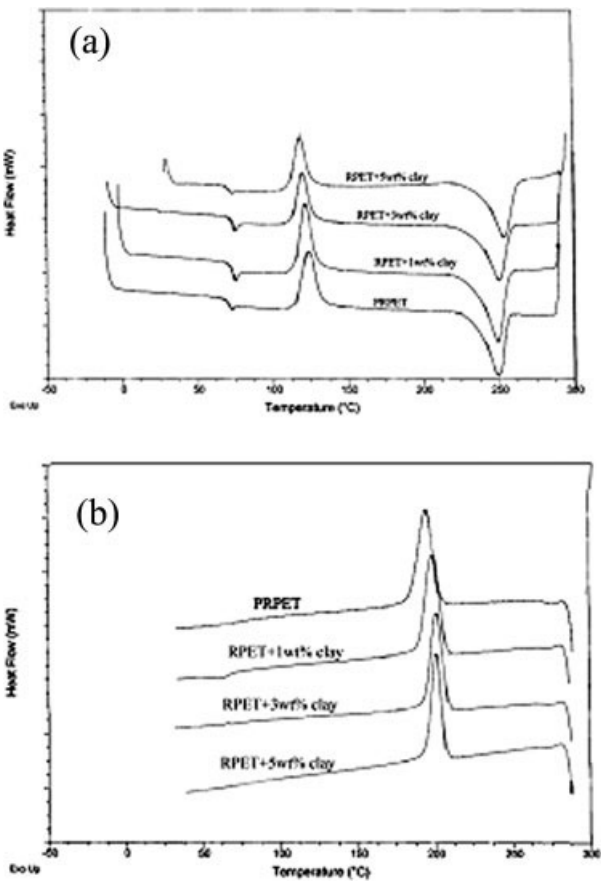

Figure 4 DSC thermograms of PRPET and RPET nanocomposites (a): Heating, (b): cooling process.

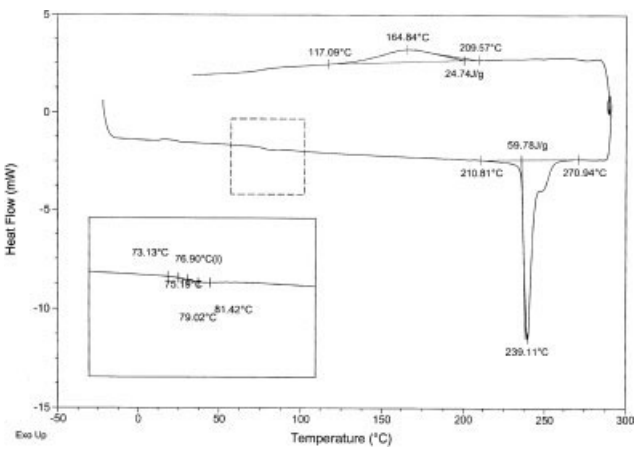

Figure 5 Heating and cooling DSC thermograms of the unprocessed virgin PET.

TABLE II
Values of Thermophysical Parameters Obtained for Different Samples by Heating and Cooling Scanning Calorimetry

Sample	T_g (°C)	T_m (°C)	ΔH_m (J/g)	T_c (°C)	ΔH_c (J/g)	X_c (%)
FPET	76.90	239.11	59.78	164.84	24.74	57.42
Processed RPET	72.21	249.29	29.77	195.15	39.81	28.59
RPET + 1 wt % clay	74.11	249.22	38.29	200.57	40.92	36.78
RPET + 3 wt % clay	73.67	249.31	39.79	202.47	42.35	38.22
RPET + 5 wt % clay	69.36	249.83	40.75	202.26	38.74	39.14

lization temperature of 209.57°C. While the cooling temperature thermograms of the RPET and the prepared nanocomposite samples show an intense exothermic crystallization peak with much higher T_c than the virgin PET. The interesting point is the significant difference between the nonisothermal crystallization behavior of the virgin PET (FPET) and its corresponding PRPET. As can be observed in Figure 4, the PRPET exhibits higher onset crystallization temperature and peak temperature (T_c) with higher crystallization enthalpy (ΔH_c). This could be explained to be the result of lower melt viscosity of the PRPET which can accelerate the chain transfer from the molten phase into the growing crystalline latices. The DSC results reveal that the overall crystallization rate for the RPET/nanocomposite samples is greater than RPET and virgin PET resins.

Comparison between thermal behavior (thermal resistance) of the virgin PET and RPET together with their corresponding nanocomposites has been demonstrated in Figures 6 and 7. It can be seen that the onset of thermal degradation has been delayed for both groups of nanocomposite PET samples. The improved thermal stability shown by the PET nanocomposites has been attributed to the shielding effects of nanoclay layers[18] as a result of high interaction between the organoclay and PET molecules together with their high heat insulation, as well as barrier function toward the volatile molecules resulting from the PET thermal decomposition.[19,20]

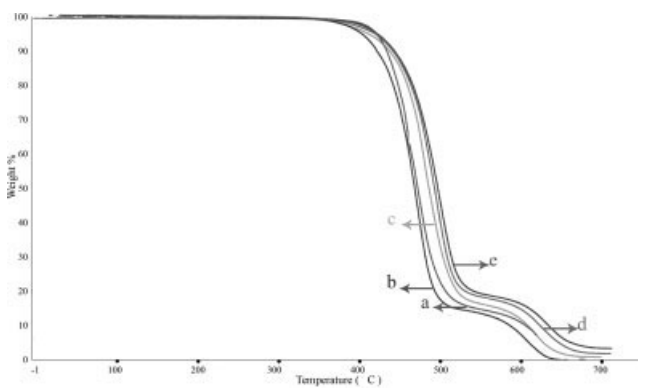

Figure 6 TGA curves of (a): virgin PET, (b): processed virgin PET, (c): virgin PET + 1 wt % clay, (d): virgin PET + 3 wt % clay, (e): virgin PET + 5 wt % clay.

Tensile properties of the PET/nanocomposites

Tensile strength and tensile modulus measured for the prepared nanocomposite PET samples have been presented and compared with the used reference PET resin samples in Figures 8 and 9 respectively. It can be seen that, for both groups of PET nanocomposite, there is an optimal nanoclay concentration for tensile strength which is 3% by weight. Below this level, tensile stress increases by raising the organoclay content, as part of the imposed stresses, are tolerated by the dispersed clay platelets. However, above the optimal clay level, high interaction between the clay layers and PET segments results in decreasing tensile strength due to the stress concentration. However, it is clearly observed that all the nanocomposite samples prepared from the RPET show higher tensile resistance, compared with those based on virgin PET resin. This is in consistence with the higher degree of exfoliated nanostructure exhibited in the XRD patterns of the RPET/nanocomposites. Lower modulus of the RPET nanocomposites is explained to be due to the lower MW (IV) for RPET than for virgin PET resin.

Melt viscoelastic characteristics

Figures 10 and 11 represent the variation of shear storage modulus (G'), loss modulus (G''), and shear

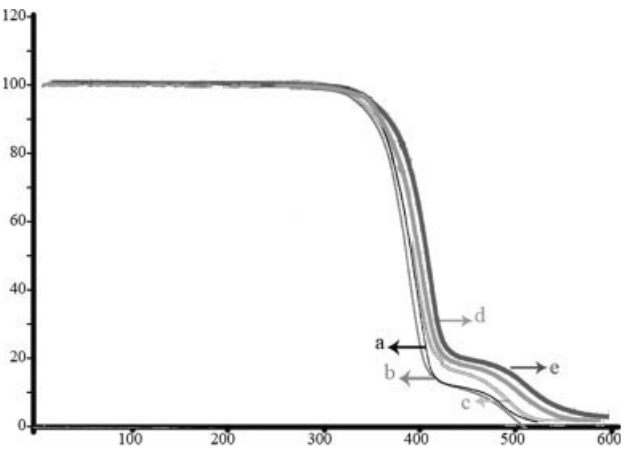

Figure 7 TGA curves of (a): RPET, (b): processed RPET, (c): RPET + 1 wt % clay, (d): RPET + 3 wt % clay, (e): RPET + 5 wt % clay.

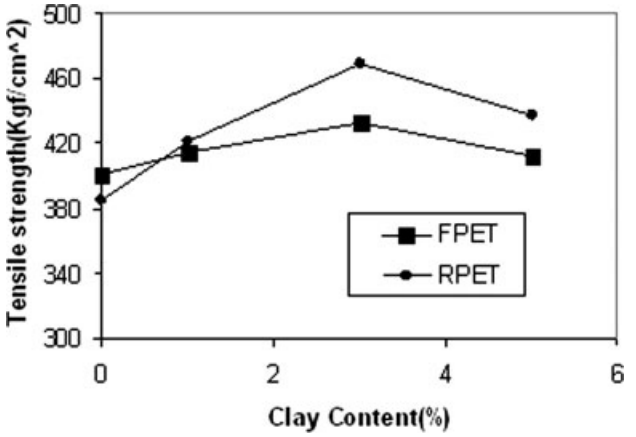

Figure 8 Tensile strength of PET and RPET nanocomposites as a function of clay content.

viscosity of the molten RPET as well as its corresponding nanocomposites prepared at various nanosilicate (DK2) loading derived from parallel plate RMS. It is clearly observed in Figure 10(a) that the nanocomposite samples composed of 3 and 5 wt % of nanoclay exhibit higher storage modulus at low shear frequency with less frequency dependency within the low shear frequency range, indicating the formation of nanoscopic network structure by the clay nanolayers. However, the sample composed of 1% nanoclay show lower storage modulus at low frequency compared with the unfilled pristine RPET, which is consistent with lower IV of the nanocomposite samples. Two factors are expected to be involved in the behavior of PET nanocomposite samples. First, the reinforcing role exerted by the intercalation/exfoliation type of morphology, and second, the thermal degradation and scission of the PET molecules which is activated by the presence of nanoclay. At low nanoclay content, the induced degradation effect of the nanoclay is predominated than its reinforcing mechanism. This is in accordance

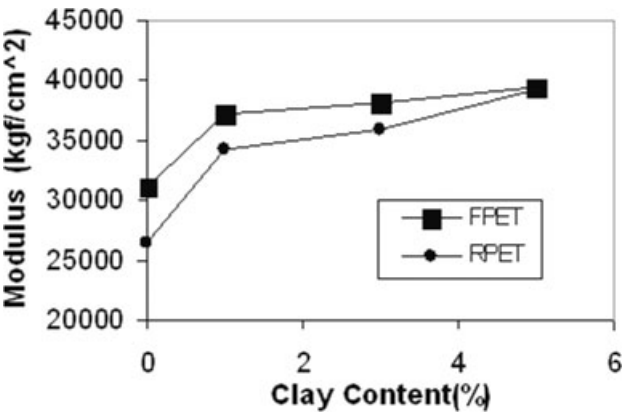

Figure 9 Tensile modulus of PET and RPET nanocomposites as a function of clay content.

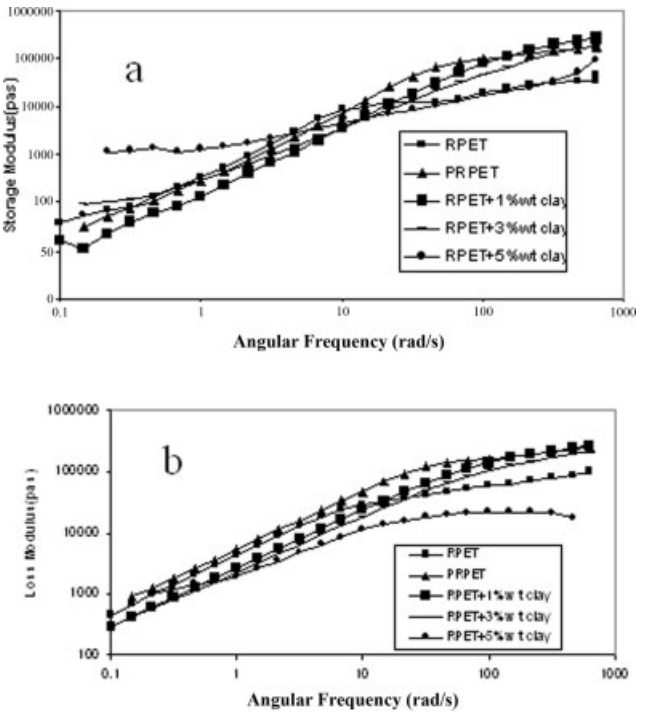

Figure 10 Variation of (a) shear storage modulus (G') and (b) shear loss modulus (G'') as a function of angular frequency for the molten RPET and its corresponding nanocomposites with various level of nanoclay at 265°C.

with the lower melt viscosity exhibited by the RPET/nanocomposite sample loaded with 1 wt % of Nanoline (Fig. 11). However, at high shear frequency, the RPET/nanocomposite sample reinforced by 1 wt % shows much higher melt elastic modulus (G') than the RPET and nanocomposites filled with 3

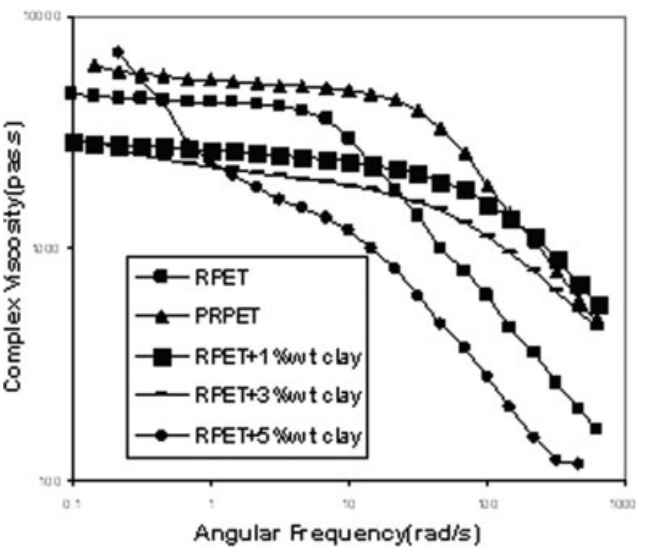

Figure 11 Variation of complex viscosity versus angular frequency for molten RPET and its corresponding nanocomposites with various level of nanoclay at 265°C, derived from rheomechanical spectroscopy.

and 5 wt %, which is attributed to the more breakdown of the PET resin filled with 3 and 5 wt % of nanoclay. Therefore, for the 1% reinforced RPET/nanocomposite, higher melt strength is expected at high melt shear processing.

In Figure 11, it is interesting to see that the melt viscosity of the RPET/nanocomposites with the nanoclay concentration lower than 5 wt % show more Newtonian behavior at low shear frequency and also less pseudoplastic characteristics within the high shear frequency region. More interesting is the significant drop in the melt viscosity of the nanocomposite sample filled with 5% of the layer silicate, which is indicative of the high physical network structure formed by the nanofiller particles as a result of percolation at concentrations above 3 wt %.

Acetaldehyde content and microbiological evaluation

The level of acetaldehyde generated during melt processing of organoclay (DK2) and RPET as a result of thermomechanical degradation of PET has been given in Table III. It is observed that the concentration of acetaldehyde measured in the RPET nanocomposite sample is lower than the unfilled processed RPET, which confirms the thermal stabilizing role of the nanoclay layers for the PET as was discussed in thermogravimetric analysis (TGA) results (Fig. 6).

The results obtained from the bacterial culture performed on the PET nanocomposite samples showed no growth and attachment for the *Escherichia coli* and *Staphylococcus aureus* bacteria's cited on the surface of the sample for 48 h. This leads to the conclusion that the presence of nanoscale layers in the PET matrix does not give any negative micibiological effects to the PET nanocomposite products.

Oxygen permeability measurement

To evaluate the gas permeability of the prepared nanocomposite samples, oxygen permeation was performed on the thin film samples with a thickness of 0.3 mm. Results have been demonstrated in Table IV. It is obviously seen that the neat processed PET show more permeability toward oxygen molecules than the film prepared from the unprocessed virgin PET. The permeation of the RPET was also found to be higher than both virgin and processed virgin PET, which is explained to be due to the lower MW of the RPET compared with the processed virgin PET, as presented in Table I. However, all the nanocomposite PET samples based on RPET exhibited lower O_2 permeability than the virgin and processed virgin PET. These results show the potentiality of the organoclay (DK2) layers to reduce the gas permeability of the RPET resin. This enables to manufacture beverages such as soft drink bottles where low permeability is desired. It is also clear that for 1% by weight of DK2 the permeability is lower than 3%, which is explained by the higher degree of nanoclay exfoliation in the structure of the nanocomposites composed of 1% organoclay (Figs. 1 and 2).

TABLE III
Acetaldehyde Content of the Prepared Nanocomposite PET Samples

Sample	Acetaldehyde content (ppm)
Processed PET	0.061
Processed RPET	0.093
PET + 3 wt % clay	0.056
RPET + 3 wt % clay	0.048

TABLE IV
O_2 Permeation of the Prepared Nanocomposite PET Samples

Sample	O_2 permeation ($cm^3\ m^{-2}\ day^{-1}\ bar^{-1}$)
FPET	25.33
Processed PET	28.14
PET + 1 wt % clay	19.60
PET + 3 wt % clay	21.70
PET + 5 wt % clay	7.890
RPET	32.40
Processed RPET	36.80
RPET + 1 wt % clay	21.80
RPET + 3 wt % clay	22.04
RPET + 5 wt % clay	8.540

CONCLUSIONS

Nanocomposite samples based on RPET soft drink bottles have been successfully prepared via melt compounding with montmorillonite modified by methyl tallow bis(2-hydroxyethyl) ammonium, with the commercial name of Nanoline (DK2). To assess the extent of reinforcement as well as improvement in various properties, a second group of nanocomposites was also prepared using unprocessed virgin PET resin from which bottles had been prepared. XRD results revealed that intercalation/exfoliation type of nanostructure is developed when DK_2 organoclay is incorporated onto the PET matrix. PET/nanocomposites showed higher tensile strength at all nanoclay concentrations, which are in accordance with the observed XRD patterns. IV of the RPET/nanocomposite was found to remain constant by increasing the organoclay content, while in the case of those based on virgin PET showed decreasing content. Dispersed clay platelets could shield the RPET from thermal degradation. Permeability of the thin films prepared from RPET/nanocomposite to oxygen gas was reduced significantly compared with

both virgin and RPET. No bacterial growth was observed for the RPET/nanocomposite samples. Nonisothermal crystallization temperature (T_c) was found to increase for all the PET/nanocomposites.

We thank the Zam Zam soft drink manufacturing company of Iran for their kind assistance during this research work.

References

1. Imai, Y.; Nishimura, S.; Abe, E.; Tateyama, H.; Abiko, A.; Yamaguchi, A.; Aoyama, T.; Taguchi, H. Chem Mater 2002, 14, 477.
2. Lin, C. C. Macromol Symp 1998, 135, 129.
3. Cimmino, S.; D'Orazio, L.; Greco, R.; Maglio, G.; Malinconico, M.; Mancarella, C.; Martuscelli, E.; Musto, P.; Palumbo, R.; Ragosta, G. Polym Eng Sci 1985, 25, 1093.
4. Coppola, F.; Greco, R.; Ragosta, G. J Mater Sci 1986, 21, 1775.
5. Karger-Kocsis, J.; Kallo, A.; Szafner, A.; Bodor, G.; Senger, Z. Polymer 1979, 20, 37.
6. Inata, H.; Matsumaro, S. J Appl Polym Sci 1985, 30, 3325.
7. Maa, C. T.; Chang, F. C. J Appl Polym Sci 1993, 49, 913.
8. Cardi, N.; Pó, R.; Gianootta, G.; Occhiello, E.; Garbassi, F.; Messina, G. J. J Appl Polym Sci 1993, 50, 1501.
9. Bikiaris, D. N.; Karaynnidis, G. P. J Polym Sci Part A: Polym Chem 1996, 34, 1337.
10. Lontjens, T.; Pawls, K.; Derks, F.; Neilen, M.; Sham, C. K.; Serné, M. J Appl Polym Sci 1997, 65, 1813.
11. Abus-Isa, I. A.; Eusebi, E.; Jaynes, C. B. U.S. Pat. 4,661,546 (1987).
12. Abus-Isa, I. A.; Eusebi, E.; Jaynes, C. B. U.S. Pat. 4,845,169 (1989).
13. Abu-Isa, I. A.; Jaynes, C. B.; Ogaro, J. F. J Appl Polym Sci 1996, 59, 1957.
14. Kim, S. W.; Jo, W. H.; Lee, M. S.; Ko, M. B.; Jho, J. Y. Polym J 2002, 34, 13.
15. Chang, J. H.; An, Y. U. J Polym Sci Part B: Polym Phys 2002, 40, 67.
16. Kato, M.; Usuki, A. In Polymer Clay Nanocomposites; Pinnavaia, T. J., Ed.; Wiley: New York, 2000; pp 97–109.
17. Pinnavala, T. J.; Beall, G. W. Polymer–Clay Nanocomposites; Wiley: United Kingdom, 2000; p 331.
18. Liu, Z.; Chen, K.; Yan, D.; J Polym Test 2004, 23, 323.
19. Chang, J. H.; Seo, B. S.; Hwang, D. H. Polymer 2002, 43, 2969.
20. Fornes, T. D.; Yoon, P. G.; Hunter, D. L.; Keskkula, H.; Paul, D. R. Polymer 2002, 43, 5915.